Int J Earth Sci (Geol Rundsch)
DOI 10.1007/s00531-009-0442-4

ORIGINAL PAPER

Zircon Hf isotope perspective on the origin of granitic rocks from eastern Bavaria, SW Bohemian Massif

Wolfgang Siebel · Fukun Chen

Received: 6 September 2008 / Accepted: 19 April 2009

Abstract The petrogenetic potential of in situ laser ablation Hf isotope data from melt precipitated zircons was explored through the analyses of about 700 individual crystals derived from about 20 different granitic intrusions covering the Variscan basement segment of eastern Bavaria, SE Germany. In combination with geochemical features, four major suites of granitic rocks can be distinguished: (1) NE Bavarian redwitzites (52–57 wt% SiO_2, intrusion ages around 323 Ma) have chondritic εHf(t) values (+0.8 to –0.4). The redwitzites are hybrid rocks and the Hf data are permissive of mixing of a mantle progenitor and crustal melts. (2) Various intermediate rock types (dioritic dyke, granodiorite, palite, 59–63 wt% SiO_2, 334–320 Ma) from the Bavarian Forest yield negative εHf(t) values between –3.4 and –5.1. These values which apparently contradict a mantle contribution fingerprint an enriched (metasomatized) mantle component that was mixed with crustal material. (3) Voluminous, major crust forming granites *sensu stricto* (67–75 wt% SiO_2, 328–298 Ma) are characterized by a range in εHf(t) values from –0.5 to –5.6. Different crustal sources and/or modification of crustal melts by various input of juvenile material can explain this variation. (4) Post-plutonic (*c.* 299 Ma) porphyritic dykes of dacitic composition (64–67 wt% SiO_2) from the southern Bavarian Forest have chondritic εHf(t) values (+0.6 to –1.1) and display large intergrain Hf isotope variation. The dykes form a separate petrogenetic group and the Hf data suggest that the zircons crystallized when a pristine mantle-derived parental melt was modified by infiltration of crustal material. The zircon Hf data form a largely coherent positive array with the whole-rock Nd data and both systems yield similar two-stage depleted mantle model ages (1.1–1.7 Ga).

Keywords Bohemian Massif · Granitoid · Hafnium isotopes · Laser ablation ICP-MS · Variscan · Zircon

Introduction

Zircon, $ZrSiO_4$, is a unique mineral in Earth sciences because it offers potential for the applicability of several different radiogenic (U–Th/Pb, U–Th/He) and stable (oxygen) isotope systems (see articles in Hanchar and Hoskin 2003). Technical developments in the last few years have made it possible to measure the Hf isotopic composition of individual zircons in situ by laser ablation ICP-MS (Thirlwall and Walder 1995) and a major recent scientific breakthrough in application of the Lu–Hf zircon system was the recovery of information about the early chemical fractionation of the Earth (Harrison et al. 2005; Hawkesworth and Kemp 2006; Scherer et al. 2007). The chemical behavior of Hf is similar to Zr and Hf forms an integral part of the zircon lattice. Zircon can incorporate ~0.4–4 wt% HfO_2 (Hoskin and Schaltegger 2003)

Electronic supplementary material The online version of this article (doi:10.1007/s00531-009-0442-4) contains supplementary material, which is available to authorized users.

W. Siebel (✉)
Institut für Geowissenschaften, Universität Tübingen,
Wilhelmstraße 56, 72074 Tübingen, Germany
e-mail: wolfgang.siebel@uni-tuebingen.de

F. Chen
Laboratory for Radiogenic Isotope Geochemistry,
Institute of Geology and Geophysics,
Chinese Academy of Sciences, 100029 Beijing, China

Published online: 12 May 2009

resulting in Lu/Hf ratios typically <0.001, much lower than the bulk Lu/Hf ratio of the continental crust. When a zircon is formed under magmatic conditions, it acquires the $^{176}Hf/^{177}Hf$ isotope composition of the melt and given the low Lu/Hf ratio, this ratio remains virtually constant through geological time. Because Hf is more incompatible than Lu during mantle melting, the melt acquires a lower Lu/Hf ratio compared to the residual mantle. As a consequence, crust and mantle show different Hf isotopic evolution with time and the $^{176}Hf/^{177}Hf$ ratio of a zircon can be used as an excellent tracer of the source material and the time of crust/mantle differentiation (Kinny and Maas 2003).

In the past few years, Hf isotope data of detrital zircons have been successfully used as a provenance indicator of sedimentary successions (e.g. Augustsson et al. 2006; Gerdes and Zeh 2006; Flowerdew et al. 2007; Li et al. 2007a, b). On the other hand, the Hf isotopic record of magmatic zircons can be useful in deciphering the sources of igneous rocks and petrogenetic processes, like magma mixing or assimilation (Griffin et al. 2002; Andersen and Griffin 2004; Belousova et al. 2006; Flowerdew et al. 2006; Goodge and Vervoort 2006; Kemp et al. 2007; Zeh et al. 2007). In this paper, we augment the latter aspect by evaluating the Hf isotopic information provided by magmatic (melt-precipitated) zircons with respect to the origin and evolution of their host magmas.

The isotopic character of the zircon can only be related to the isotopic character of the melt if no pre-magmatic (inherited) zircon component was present during crystallization. To illuminate the magma generation process, we have selected samples with zircon populations largely absent in inherited material. Evidence for the inheritance-free nature of these populations had been gained from earlier U–Pb and Pb–Pb analyses and from detailed cathodoluminescence studies of each analyzed grain. Our purpose was (1) to document the isotopic variability of the melt from which the zircons crystallized and (2) to draw conclusions about the relative contribution of pre-existing crustal and newly added mantle-derived sources in their genesis and (3) to contribute to the identification and characterization of different magma systems or evolutionary/petrogenetic processes. In detail, we present 700 Hf measurements from inheritance-free magmatic zircons comprising *c.* 20 late-Variscan igneous rocks of the SW Bohemian Massif. These granitoids are appropriate candidates for such investigation because most of them are well-dated and composed of different rock types (containing crust- and mantle-derived components) with well-documented chemical and isotopic composition. This also allows comparison between the Hf zircon system and other isotope tracers like the Nd bulk rock isotope system.

Geology

Variscan granitoids form an integral component in terms of volume and areal extent within the SW Bohemian Massif. They were emplaced in different thrust-bound geological units, or micro plates (Moldanubian, Saxothuringian, Teplá-Barrandian), all part of the Armorican Terrane Assemblage (for geodynamic plate models see Franke 2000; Tait et al. 2000; Kroner et al. 2007). The granitoids can be subdivided according to different petrogenesis, composition and age (e.g. Holub et al. 1995). Older, lower-Carboniferous subduction-related magmatism played a role during the formation of the calc-alkaline Central Bohemian batholith (*c.* 354–336 Ma, Janoušek and Gerdes 2003; Žák et al. 2005). The majority of granitoids within the SW Bohemian Massif (e.g. South Bohemian batholith and numerous northwest extending plutons) formed in a late to post-orogenic setting, i.e. in a setting unrelated to subduction-collision processes. A final episode of metamorphism and anatexis affected the previously thickened lower Variscan crust of the SW Bohemian Massif during the Late Visean (Kalt et al. 2000; Finger et al. 2007) and abundant late to post-orogenic granitoids formed during this high crustal-heat flow event (Klein et al. 2008; Siebel et al. 2008). Based on mineralogical characteristics, these granitoids can be subdivided into (1) prevalent masses of amphibole-free peraluminous biotite and two-mica granites and (2) minor group(s) of metaluminous (amphibole-bearing) granitoids. They occupy the *c.* 250 km long westernmost margin of the Bohemian Massif along the boundary between Germany and the Czech Republic (Fig. 1). The rocks were emplaced at different crustal depths, likely into the deeper, poly-metamorphic rocks of the Moldanubian unit (migmatites, para- and orthogneisses) in the southeast and into upper, low-grade Saxothuringian unit (metasediments and minor orthogneisses and metavolcanics) in the northwest (e.g. Klein et al. 2008).

Late- to post-orogenic extension of the Variscan mountain belt is documented by extensional movements along faults or by the formation of intramontane troughs and sedimentary basins. A post-plutonic phase linked to late-Variscan lithospheric extension is recorded by mafic to intermediate dykes that intruded the granitoids and migmatite complex of the SE Bavarian Forest (Propach et al. 2008).

Analytical techniques

The whole rock samples, from which zircons were separated, were analyzed for major and trace elements by X-ray fluorescence (XRF). The samples were crushed and split, and *c.* 100 g representative material was pulverized in an

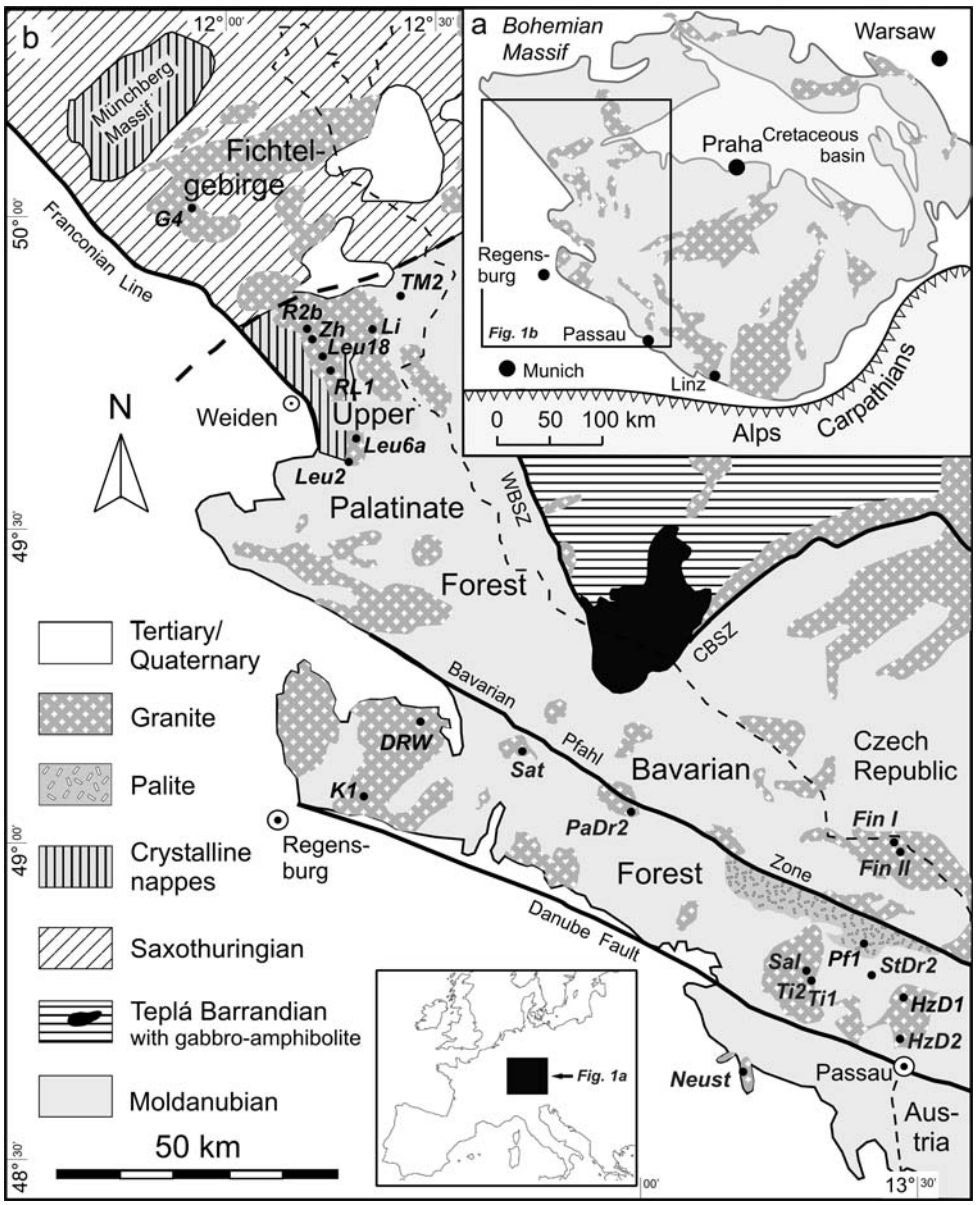

Fig. 1 **a** Schematic map showing the position of the Bohemian Massif north of the Alpine belt in central Europe with study area (outlined). **b** Geological map of the western margin of the Bohemian Massif featuring the distribution of Variscan granites and showing sample locations (*dark circles*). *CBSZ* central Bohemian shear zone, *WBSZ* west Bohemian shear zone

agate mill. The powdered samples were dried at 105°C before loss on ignition (LOI) was determined gravimetrically at 1,050°C. Major and trace elements were determined on fused lithium tetraborate glass beads by wavelength dispersive techniques. The precisions of major elements are typically better than 2%, except for P and Mn which have precisions better than 15%. The precision for a given trace element is better than 5–10%.

Zircons were extracted from the whole-rock samples using standard techniques of density and magnetic separation, handpicked under a binocular microscope, mounted in epoxy and polished to expose the centers of the grains.

In situ zircon Hf isotopic analyses were carried out at the Institute of Geology and Geophysics, Chinese Academy of Sciences, using a Neptune MC-LA-ICPMS with an ArF eximer laser ablation system. Analytical techniques have been recently described in detail by Wu et al. (2006) and the reader is referred to this paper for further information on measurement procedures and interference correction. Isotope analyses were performed on zircons monitored by cathodoluminescence (CL) studies, and the CL images provided guidance in the choice of grains and the beam spot sites. Beam diameters of 63 μm were used for different samples and the pulsed laser repetition rate was kept to 10 Hz. The signal intensities of zircon ^{180}Hf were generally higher than 5.5 V. Isobaric interference of ^{176}Lu on ^{176}Hf was corrected using the intensity of the interference-free ^{175}Lu isotope and a recommended ^{176}Lu/^{175}Lu ratio of 0.02655 (Machado and Simonetti 2001). Isobaric interference of ^{176}Yb on ^{176}Hf was

corrected using the mean fractionation index proposed by Iizuka and Hirata (2005). It was suggested that this method provides accurate correction for in situ Hf isotope composition of zircons (Wu et al. 2006). For our instrument, a $^{176}Yb/^{172}Yb$ ratio of 0.5887 was obtained for zircon 91500 (Wu et al. 2006) identical with previously reported data (Chu et al. 2002; Vervoort et al. 2004) and this ratio was applied for Yb correction. Zircon 91500 was used as the reference material during data acquisition. Forty-nine analyses of this standard yielded a $^{176}Hf/^{177}Hf$ weighted mean value of 0.282326 ± 35 (2-sigma standard deviation). Hafnium isotope ratios are reported relative to a $^{176}Hf/^{177}Hf$ value of 0.282306 obtained by solution ICPMS on standard zircon 91500 (Woodhead et al. 2004). The JMC 475 standard solution was used for evaluating the reproducibility and accuracy of the instrument and the results of this standard as well as our in-house standard solution JMC14374 are published in Wu et al. (2006).

εHf(t) values were calculated using the new chondritic Hf data of $^{176}Hf/^{177}Hf = 0.282785$ and $^{176}Lu/^{177}Hf = 0.0336$ (Bouvier et al. 2008). Uncertainty of the εHf values based on standard (91500) zircon reproducibility is ±1.1 ε-units. A value of 1.865×10^{-11} per year (Scherer et al. 2001), corresponding to a half-life of 37.2 billion years, was used for the decay constant of ^{176}Lu.

Because of the low Lu/Hf ratio of zircon, a model age calculated from the measured $^{176}Hf/^{177}Hf$ and $^{176}Lu/^{177}Hf$ ratios of a zircon would give only a minimum limit for the crustal residence age of the hafnium in the zircon. In this study, Hf model ages, Hf T_{DM}, were calculated using the measured $^{176}Lu/^{177}Hf$ of the zircon to determine the $^{176}Hf/^{177}Hf$ ratio at the time of crystallization. Based on the Lu/Hf bulk crust estimate of 0.081 (Rudnick and Gao 2003), and the present-day isotope composition of Lu and Hf, a mean crustal $^{176}Lu/^{177}Hf$ value of 0.0113, was employed to further trace back this ratio through time and to determine the intersection with the average depleted mantle evolution curve. The dependence on the choice of the Lu/Hf ratio ranging from more mafic (e.g. $^{176}Lu/^{177}Hf = 0.022$) to more felsic (e.g. $^{176}Lu/^{177}Hf = 0.0093$, Vervoort and Patchett 1996) ratios was recently discussed by Nebel et al. (2007). For reconstructing the depleted mantle evolution curve, we have chosen present-day isotope parameters of $^{176}Hf/^{177}Hf = 0.28325$ and $^{176}Lu/^{177}Hf = 0.0384$ (Griffin et al. 2000), which are similar to those that were reported for average mid-ocean ridge basalts (e.g. Chauvel and Blichert-Toft 2001).

The newly presented Nd whole-rock isotopic compositions were determined using isotope dilution thermal ionization mass spectrometry (ID-TIMS) techniques at the Institute of Geosciences, Tübingen. After spiking with a mixed ^{149}Sm-^{150}Nd spike, the samples were dissolved in hydrofluoric acid at 180°C in pressure digestion bombs. Details of the chromatographic separation of Sm and Nd are given by Siebel et al. (2008). Isotopic data were obtained in static multiple collector mode on a Finnigan MAT 262 mass spectrometer. The $^{143}Nd/^{144}Nd$ ratios were normalized to $^{146}Nd/^{144}Nd = 0.7219$. Repeated measurements of the La Jolla Nd standard ($n = 12$) gave a $^{143}Nd/^{144}Nd$-ratio of 0.511838 ± 13 (errors are $\pm 2\sigma$ of the mean). Blanks were <90 pg for Nd and <20 pg for Sm. Depleted mantle Nd model-ages (Nd T_{DM}) were calculated according to the two-stage approach with parameters given in Liew and Hofmann (1988) and εNd(t) values were calculated using new present-day CHUR parameters (Bouvier et al. 2008: $^{147}Sm/^{144}Nd = 0.1960$, $^{143}Nd/^{144}Nd = 0.512630$).

Granitoid types, petrography, geochemistry and geochronology

Figure 1 depicts the distribution of late-Variscan igneous rocks at the western margin of the Bohemian Massif and shows the location of samples investigated in this study. The area covers the Fichtelgebirge (Saxothuringian unit), the Upper Palatinate Forest (transition from Saxothuringian to Moldanubian unit, including Teplá-Barrandian/Bohemian nappes) and the Bavarian Forest (Moldanubian unit).

Samples can be divided into four distinct igneous rock types (Fig. 2)

(1) A suite of mineralogically heterogeneous biotite and hornblende bearing quartz monzodiorites and granodiorites has geochemical characteristics that fit the I-type classification (White and Chappell 1977). Such rocks, referred to as *redwitzites* (Willmann 1920; Troll 1968), occur in the Fichtelgebirge, Upper Palatinate Forest and western Bohemia (Siebel et al. 2003; Kováříkova et al. 2007). Field and geochemical observations highlight the importance of mixing between mafic (gabbroic) and felsic (granitic) magmas in the formation of the redwitzites. Mixing and hybridisation models were also established in earlier studies to explain the variation in initial Sr and Nd isotope ratios (Holl et al. 1989; Siebel 1994). Redwitzites investigated in this study are strongly metaluminous, with high Mg, Ca, Fe and Ti concentrations (Table 1). Two of the samples targeted for this study yield zircon $^{207}Pb/^{206}Pb$ evaporation ages of 323 ± 3 Ma (sample RL1) and 323 ± 4 Ma (sample R2b) (Siebel et al. 2003), interpreted as the time of magmatic emplacement of the redwitzite group.

(2) Granitoids of monzonitic/granodioritic composition are also present further south in the Bavarian Forest but these rocks differ in several respects from the redwitzites. They are hereafter referred to as intermediate granitoids. A complex of strongly foliated coarse-grained, inequigranular

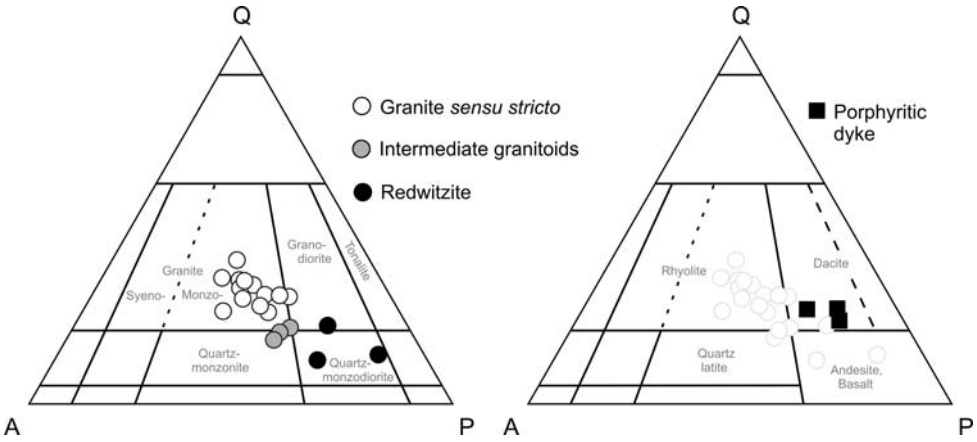

Fig. 2 Modal classification of the investigated samples according to the QAP (quartz-alkali feldspar-plagioclase) diagram (Streckeisen 1976) for plutonic and (sub)volcanic rocks

Table 1 Whole-rock compositions of samples from redwitzites, intermediate granitoids and porphyritic dykes

Sample	Redwitzite			Intermediate granitoid			Porphyritic dyke		
	TM2	R2b	RL1	DRW	PaDr2	Pf1	HzD2	HzD1	StDr2
SiO_2	51.59	55.21	57.07	59.41	62.44	62.65	64.02	65.65	66.61
TiO_2	1.39	1.52	1.19	1.40	1.20	0.79	0.69	0.52	0.41
Al_2O_3	17.17	17.39	16.19	16.45	16.36	16.77	17.06	17.02	16.29
Fe_2O_3	8.06	7.21	7.09	6.45	6.03	4.64	3.83	3.13	2.58
MnO	0.12	0.12	0.11	0.09	0.09	0.07	0.06	0.06	0.04
MgO	7.49	3.22	5.07	1.93	1.96	2.44	1.95	1.53	1.17
CaO	7.22	6.60	5.46	3.49	3.78	3.64	4.10	3.61	3.04
Na_2O	2.87	2.76	3.23	4.16	3.41	3.63	4.23	3.91	3.41
K_2O	2.81	3.35	3.28	4.73	4.39	4.49	2.73	2.69	3.40
P_2O_5	0.61	0.47	0.37	0.72	0.43	0.32	0.23	0.17	0.15
LOI	1.15	1.37	1.02	1.45	0.69	0.92	0.74	1.03	1.43
Total	100.5	99.3	99.6	99.7	100.8	100.4	99.8	99.8	99.2
Ba	2,283	1,188	1,140	1,221	1,335	1,178	763	648	945
Rb	123	119	124	187	140	146	77	83	69
Sr	703	591	375	365	329	447	708	568	558
Y	31	26	27	66	52	21	16	13	13
Zr	225	322	244	699	595	266	188	172	181
La	29	62	56	82	68	34	48	45	37
Ce	102	131	117	216	182	76	85	60	70
Nd	46	49	42	98	77	37	26	28	23
Sm	6.7	8.5	7.3	17.2	13.5	4.7	5.8	3.3	4.2

Major elements in wt%, trace elements in ppm

– not determined, *LOI* Loss on ignition

granitoids with K-feldspar megacrysts occupies a 5–7 km wide and approximately 50 km long stripe along the Bavarian Pfahl zone (Fig. 1). The term *palite* was introduced by Frentzel (1911) for these rocks. The crystallization age of the investigated palite sample (Pf1, $^{207}Pb/^{206}Pb$ evaporation age: 334 ± 3 Ma, U–Pb ages: 327–342 Ma, Siebel et al. 2005) is consistent with a pre-high-temperature metamorphic emplacement time of these rocks. In the northwestern prolongation of the palite zone, a geochemically and mineralogically similar but undeformed granodiorite body crops out that was targeted (sample PaDr2). The age of the granodiorite was determined at 325 ± 3 Ma (concordant U–Pb ages, Siebel et al. 2006a). Another dioritic rock type occurs as small masses such as dykes and sills, which intrude the Kristallgranit (K1) and paragneisses of the NW Bavarian Forest. These dykes range in

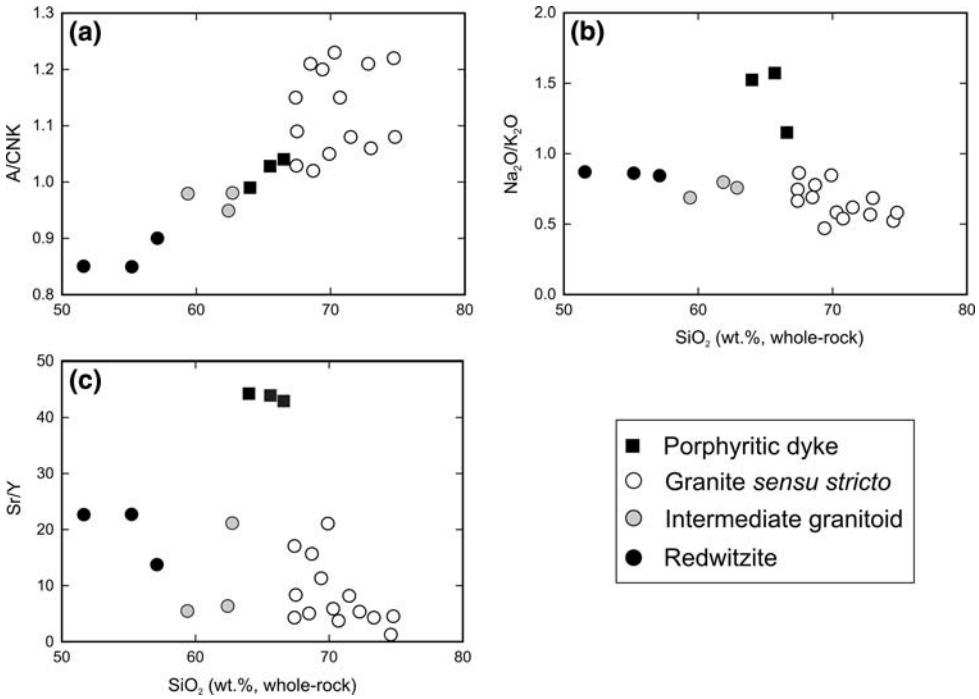

Fig. 3 Harker-type diagrams for whole-rock data of the 23 investigated samples. A/CNK = molar Al_2O_3/($CaO + K_2O + Na_2O$) ratio

composition from diorite sensu stricto to granodiorite (Köhler and Müller-Sohnius 1986 and references therein). Our sample (DRW, Fig. 1) is a diorite and was dated by U–Pb zircon analysis at 322 ± 5 Ma (author's unpublished data) considered as representing the emplacement age of the dyke. Major oxide and trace element characteristics of the samples from the intermediate granitoids are transitional between the redwitzites and the granites sensu stricto (Fig. 3).

(3) All granites sensu stricto investigated in this study are monzogranites with some compositions close to the granodiorite field (Fig. 2). Based on geochemical characteristics, they can be classified as weakly peraluminous biotite-granites (granites of Leuchtenberg, Zainhammer, Tittling) and moderately to strongly peraluminous biotite ± muscovite granites (Kristallgranit, granites of Finsterau, Sattelpeilnstein, Neustift, Saldenburg, Liebenstein, Tin granite). The latter group displays petrographic and geochemical features of S-type granitoids. The granites sensu stricto are distinct from the other plutonic units in their lack of hornblende, high K_2O/Na_2O ratios, and high Al and low Ca contents (Fig. 3). They can be divided into different age groups. The first age group (328–320 Ma) comprises the granites of Leuchtenberg, Zainhammer, Tittling, K1, Finsterau and Sattelpeilnstein whereas the second group (315–312 Ma) includes the Saldenburg and Liebenstein granites. The Tin granite (G4) from the Fichtelgebirge intruded during a distinctly younger event at 298 ± 3 Ma (mean zircon $^{207}Pb/^{206}Pb$ evaporation age, author's unpublished data). The crystallization age of the Neustift granite has not yet been successfully determined by U–Pb or Pb–Pb dating of zircon; in analogy to similar well-dated granites in this part of the Bavarian Forest (Siebel et al. 2008), a crystallization age of 320 Ma is assumed for this intrusion. For compilations of published age data, see Chen and Siebel (2004), Klein et al. (2008), Siebel et al. (2003) and Siebel et al. (2008).

(4) In the southern Bavarian Forest, the granites and gneisses are cut by porphyritic dykes, which form a continuous series from basaltic andesite to dacite (Propach et al. 2008). According to the QAP classification, the three samples investigated in this study are dacites (Fig. 2). The rocks contain amphibole and biotite as mafic phenocrysts and display slightly metaluminous to peraluminous compositions. Their sodium-rich composition and prevalence of Na over K signals some A-type affinity and the high Sr/Y ratios suggest that the melt equilibrated with a garnet-bearing residue (Fig. 3). One of the dykes (HzDr2) was dated by U–Pb geochronology and the young age (299 ± 2 Ma, Propach et al. 2008) is in agreement with an emplacement in a post-plutonic extensional tectonic setting.

Results

Major and trace elements of the samples from which zircons were analysed are presented in Tables 1 and 2. The Lu–Hf isotope composition for 700 zircons extracted from 23 samples is summarized in Table 3, organized by rock

Table 2 Whole-rock composition of samples from granites sensu stricto

Sample	Zh	Leu18	Fin I	K1	Ti1	Li	Ti2	Fin II	Sat	Leu6a	Neust	Sal	G4	Leu2
SiO_2	67.37	67.42	67.54	68.53	68.7	69.39	69.9	70.28	70.74	71.47	72.81	73.0	74.71	74.80
TiO_2	0.48	0.56	0.68	0.44	0.43	0.26	0.43	0.33	0.44	0.36	0.28	0.38	0.10	0.13
Al_2O_3	15.90	15.43	15.65	15.50	14.85	16.51	15.16	15.14	14.80	14.01	14.52	13.68	13.27	13.09
Fe_2O_3	3.14	3.41	3.77	2.94	3.25	1.67	2.58	2.16	2.63	2.55	1.48	2.49	1.73	1.12
MnO	0.05	0.06	0.05	0.04	0.06	0.03	0.05	0.02	0.04	0.06	0.02	0.04	0.03	0.03
MgO	0.69	0.84	1.19	0.77	0.89	0.77	0.89	0.65	0.70	0.47	0.48	0.47	0.07	0.21
CaO	1.32	2.23	2.24	0.85	2.41	0.71	2.46	0.87	1.00	1.48	0.54	1.42	0.44	0.63
Na_2O	3.47	3.52	3.54	3.50	3.34	3.15	3.38	3.07	3.09	3.02	3.11	3.19	2.79	3.14
K_2O	5.22	4.72	4.10	5.07	4.29	6.70	3.99	5.26	5.48	4.88	5.48	4.66	5.08	5.40
P_2O_5	0.27	0.21	0.25	0.31	0.16	0.28	0.16	0.27	0.30	0.14	0.30	0.17	0.19	0.04
LOI	1.18	1.02	0.99	1.38	0.48	1.16	0.75	1.21	0.52	1.06	0.73	0.50	1.14	1.00
Total	99.4	99.4	100.2	99.5	99.1	100.8	99.90	99.4	99.9	99.5	99.9	99.8	99.6	99.6
Ba	751	1,001	918	593	1,037	707	1,016	406	436	662	372	478	62	232
Rb	253	181	225	270	153	306	252	270	335	201	309	201	575	206
Sr	129	256	192	126	376	147	569	88	97	172	70	150	7	59
Y	30	15	23	25	24	13	27	15	26	21	14	31	14	13
Zr	211	307	275	222	160	140	179	162	250	229	146	305	83	88
La	–	65	53	33	–	24	–	40	38	65	25	–	–	22
Ce	66	132	133	84	–	64	–	97	94	133	60	–	35	51
Nd	–	45	58	29	28	24	28	36	44	46	25	55	–	20
Sm	–	7.5	9.4	4.2	5.4	5.8	5.4	8.7	6.5	8.2	4.1	8.9	–	4.6

Major elements in wt%, trace elements in ppm

– not determined, *LOI* loss on ignition

types as described above. Hf isotope analyses for the complete data set are provided as an electronic supplementary data file. Nd isotope composition (Table 3) was established during the course of this study or compiled from published sources (Chen and Siebel 2004; Siebel et al. 1995, 2005, 2006a, 2008). As expected for zircons, average $^{176}Lu/^{177}Hf$ ratios are very low, ranging from 0.00072 to 0.00286 for the different samples. Thus, following the time of zircon crystallization, there was virtually no change in the zircon $^{176}Hf/^{177}Hf$ ratios but a relatively strong change in εHf values due to the increase of the chondritic $^{176}Hf/^{177}Hf$ ratios over this period; this is seen by the differences between the εHf(0) and εHf(t) values. Fig. 4 shows the εHf(t) ratios ordered from the highest (most radiogenic) to the lowest (least radiogenic) values together with the standard deviation which monitors the dispersion (i.e. scatter) of the data. The most pronounced differences in Hf isotope parameters appear with respect to various rock types and these can be summarized as follows:

Redwitzites and porphyritic dykes have the highest $^{176}Hf/^{177}Hf(t)$ ratios (mean values ranging from 0.28256 to 0.28261). As a whole, the samples of both groups have uniform Hf isotope compositions with mean initial εHf values from +0.8 to −1.1 (Table 3; Fig. 4). Large spread of data occurs in the porphyritic dykes as seen by the large standard deviation, in particular, for samples HzD1 and StDr2 (Table 3).

Zircon grains from the intermediate granitoids unit have unradiogenic Hf ratios (mean $^{176}Hf/^{177}Hf(t)$ from 0.28244 to 0.28249 and mean initial εHf values from −3.4 to −5.1). Although these rocks clearly differ from the granite group with respect to their geochemical composition (see Fig. 3), their Hf isotope compositions overlap those of this group (Fig. 4).

Zircons from the granites sensu stricto show a variation in Hf isotopic composition, from high mean $^{176}Hf/^{177}Hf(t)$ ratios around 0.28256 in the Leuchtenberg and Zainhammer granites, to low mean $^{176}Hf/^{177}Hf(t)$ ratios around 0.28242 in the Finsterau II granite. This range corresponds to a total variation of about five ε-units [εHf(t) = −0.5 to −5.6]. On the basis of the Hf values, the granites can be classified in two different groups as follows: one group is characterized by more radiogenic ratios [εHf(t) –0.5 to –1.9, Leuchtenberg, Zainhammer, Tittling, Saldenburg], the other group comprises granites with less radiogenic Hf isotope composition [εHf(t) –2.9 to –5.6, Finsterau I, Liebenstein, Sattelpeilnstein, Neustift, Kristallgranit, Tin granite, Finsterau II].

For the Leuchtenberg and Tittling granites, more than one sample was analysed in order to obtain information

Table 3 Laser ablation Hf isotope data from zircons of granitoids from eastern Bavaria

Sample no.	Age (Ma)	$^{176}Lu/^{177}Hf$	$^{176}Hf/^{177}Hf(t)$ (StdDev)	εHf(t) (StdDev)	εNd(t)	Hf T_{DM}	Nd T_{DM}
Porphyritic dyke							
StDr2 (38)	299	0.00135	0.282565 (0.000146)	−1.12 (5.14)	−2.4*	1.22	1.27
HzD1 (32)	299	0.00158	0.282602 (0.000122)	0.16 (4.32)	−0.3*	1.15	1.10
HzD2 (31)	299	0.00172	0.282613 (0.000068)	0.56 (2.44)	−0.6*	1.12	1.12
Granite sensu stricto							
Fin II (38)	324	0.00125	0.282423 (0.000098)	−5.60 (3.44)	−7.2	1.48	1.67
G4 (17)	298	0.00105	0.282470 (0.000056)	−4.53 (1.98)	−7.0*	1.40	1.63
K1 (30)	325	0.00146	0.282456 (0.000072)	−4.42 (2.56)	−6.0*	1.42	1.57
Neust (24)	320	0.00139	0.282464 (0.000100)	−4.24 (3.56)	−5.3*	1.40	1.51
Sat (20)	322	0.00119	0.282482 (0.000096)	−3.56 (3.42)	−5.8	1.37	1.55
Li (27)	315	0.00180	0.282499 (0.000096)	−3.13 (3.36)	−6.4*	1.34	1.59
Fin I (36)	326	0.00116	0.282498 (0.000054)	−2.92 (1.92)	−5.4	1.34	1.52
Sal (25)	312	0.00143	0.282536 (0.000048)	−1.86 (1.70)	−3.6	1.27	1.36
Ti2 (33)	322	0.00160	0.282538 (0.000070)	−1.58 (2.50)	−3.7	1.26	1.38
Ti1 (21)	324	0.00155	0.282539 (0.000062)	−1.50 (2.18)	−3.8	1.26	1.39
Leu18 (42)	323	0.00173	0.282544 (0.000064)	−1.33 (2.30)	−2.7*	1.25	1.30
Leu2 (28)	324	0.00286	0.282553 (0.000070)	−1.00 (2.46)	−2.8	1.23	1.32
Zh (23)	321	0.00246	0.282564 (0.000094)	−0.68 (3.32)	−3.0*	1.21	1.33
Leu6a (39)	328	0.00156	0.282566 (0.000060)	−0.49 (2.14)	−2.8	1.20	1.32
Redwitzite							
RL1 (39)	323	0.00206	0.282572 (0.000050)	−0.37 (1.74)	−0.4	1.19	1.11
TM2 (26)	323	0.00128	0.282580 (0.000088)	−0.05 (3.08)	−1.1*	1.18	1.20
R2b (26)	323	0.00229	0.282603 (0.000066)	0.75 (2.30)	−1.6	1.13	1.27
Intermediate granitoid							
DRW (30)	322	0.00261	0.282440 (0.000108)	−5.08 (3.82)	−5.1*	1.45	1.49
Pf1 (37)	334	0.00092	0.282478 (0.000070)	−3.43 (2.46)	−4.4	1.37	1.45
Padr2 (25)	325	0.00072	0.282491 (0.000056)	−3.17 (1.96)	−5.1	1.35	1.50

Number of zircons analysed is given in parentheses behind the sample no. Nd isotope whole-rock data are shown for comparison. StdDev = 2σ standard deviation (95.4% probability)

Data sources for granitoids crystallization ages (column two) used for calculation of initial Hf–Nd parameters: *porphyritic dykes* Propach et al. (2008), *granites sensu stricto* Chen and Siebel (2004), Klein et al. (2008), Siebel et al. (2003, 2008); *redwitzites* Siebel et al. (2003); *intermediate granitoids* Siebel et al. (2005, 2006a)

εNd(t) values obtained during this study are marked with an asterisk (*). References for Nd data obtained in previous studies are Chen and Siebel (2004) for samples Sal, Ti1 and Ti2, Siebel et al. (1995) for samples RL1, R2b, Leu2 and Leu6a, Siebel et al. (2005) for sample Pf1, Siebel et al. (2006a) for sample PaDr2, Siebel et al. (2008) for samples Sat, Fin I and Fin II

about the isotopic variability within single intrusions. Analyses of three different samples from the Leuchtenberg granite give virtually identical results yielding initial εHf values of –0.49 (2.14) (2-sigma SD), –1.00 (2.46) and –1.33 (2.30). A striking uniformity of initial zircon Hf isotopic composition is also observed in two different samples from the Tittling granite showing εHf(t) values of –1.50 (2.18) and –1.58 (2.50).

Zircon Hf model ages, Hf T_{DM}, are compared with whole-rock Nd depleted mantle model ages, Nd T_{DM} in Table 3. Both Lu–Hf zircon and Sm–Nd whole-rock systems yield similar model age information and are indistinguishable within their uncertainties. Zircons from the granites and intermediate granitoids yield Hf–Nd model ages generally between 1.3 and 1.7 Ga. Hf–Nd model ages of the redwitzites and porphyritic dykes are younger (1.1–1.3 Ga), consistent with a higher contribution of mantle, or less ancient crustal material in their sources.

Discussion

Hf isotopes and magma source variation

The zircons analysed in the present study are from igneous rocks generated episodically over a timescale of *c*. 35 Ma, from Viséan to Stephanian, but we found no systematic variation of initial $^{176}Hf/^{177}Hf$ ratios with age. On the other

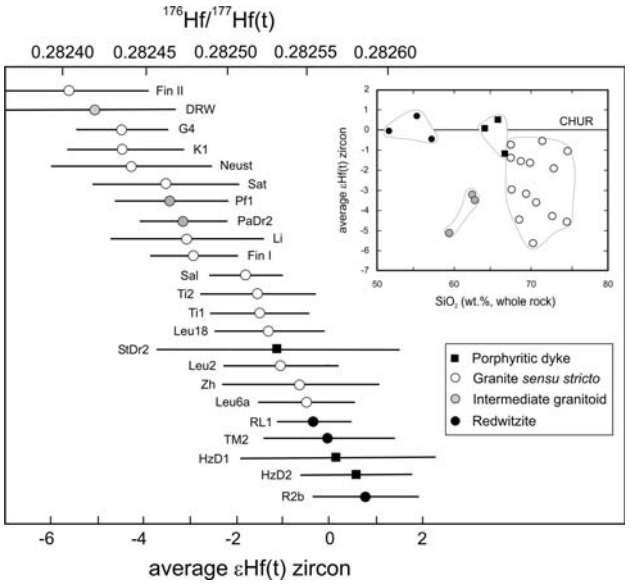

Fig. 4 Summary of Hf isotope composition of melt-precipitated zircons ordered from most (*bottom*) to least (*top*) radiogenic. Each data point represents the mean initial εHf(t) value; *error bars* denote the 1σ standard deviation. For number of zircons analysed see Table 3. *Inset* εHf(t) zircon against SiO_2 concentration of the corresponding whole-rock sample

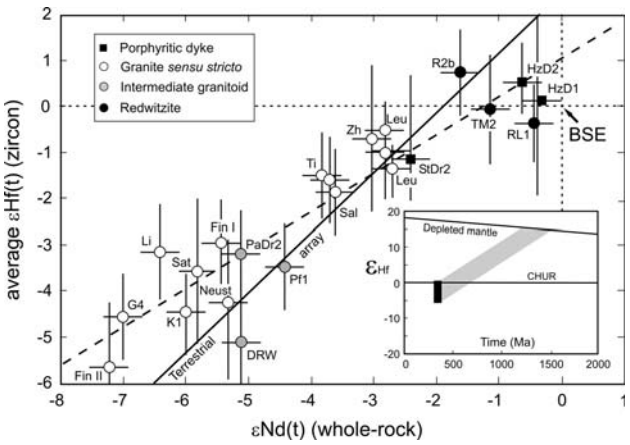

Fig. 5 Plot of εHf(t) values of melt-precipitated zircons versus εNd(t) whole-rock values in Bavarian granitoids at the time of crystallization. Terrestrial array (*solid trend line*) from Vervoort et al. (1999) recalculated, using the new decay constant of 1.865×10^{-11} y^{-1} for ^{176}Lu (Scherer et al. 2001). The data for the granitoids from eastern Bavaria do not plot along this line but require a line with a shallower slope (*the dotted line* shows the best-fit linear regression through this data). The analytical uncertainty in εNd is about 0.5 epsilon units (2σ). For *error bars* of εHf, see Fig. 4. *Inset* Projection of the initial εHf values to the depleted mantle Hf evolution curve (Griffin et al. 2000; Chauvel and Blichert-Toft 2001), depicting the range of Hf model ages for Bavarian granitoids

hand, a clear correlation does exist between the Hf and Nd isotope parameters (Fig. 5). Nd isotope composition was acquired by digestion of whole-rock samples, i.e. by conventional bulk rock analyses. The Hf–Nd array is bracketed between a crustal end-member with low ε-values [εHf(t) around –6, εNd(t) around –7] and a relatively primitive component with ratios close to the chondritic values. The trend defined by the Bavarian granitoids deviates from the terrestrial Hf–Nd array (Vervoort et al. 1999) and requires a line with a shallower slope ($\varepsilon Hf = 0.83\varepsilon Nd + 1.02$, Fig. 5). This offset must be regarded with some caution since the total range in ε-values and the number of samples in the Bavarian data set is small, compared to that in the terrestrial array. However, the reason for this offset could lie in the fact that the Bavarian samples represent a limited range in age and lithologies or do not simply constitute a binary mixing trend.

Figures 4 and 5 depict the average Hf and Hf–Nd isotope composition of the individual granitoids. Zircons from granites sensu stricto show considerable variations in Hf (five ε-units) and Nd isotope ratios extending from more mantle-like values to more crustal-like values. Potential source lithologies for the granites from the Bavarian Forest are Moldanubian paragneisses and anatexites. On the basis of bulk-geochemistry and Sr-Nd isotope composition, it has been proposed that the S-type granites, equivalent to the granites with low Hf zircons of this study, were produced by partial melting of such lithologies (Siebel et al. 2006b). The origin of the high εHf granites is less well-constrained. Their isotope signatures are appropriate for contribution of mantle-derived melts or pre-existing mafic crust. Alternatively, melts of the more mafic Teplá-Barrandian/Bohemian crust may have been involved in granite genesis (Siebel et al. 1997). Such units occur in the Saxothuringian/Moldanubian transition zone and could be potential source components for some of the granites in this region (e.g. Leuchtenberg, Zainhammer).

The intermediate granitoids are characterized by comparatively low εHf(t) values. Melt contribution from the mantle accords with the mafic character of these rocks. The Hf data are also permissive for interaction with an enriched supracrustal component. Further emphasis is needed to determine the conditions how this was achieved. The deformed granodiorites (palites) were recently interpreted as the southwestern extension of enriched shoshonitic rocks (durbachites) from central Bohemia (Finger et al. 2007). It was assumed by these authors that this enrichment took place in a supra-subduction zone. Although there is no evidence for an enriched mantle at this time in other parts of the study area (see discussion below) this event might have enriched part of the mantle below the Bavarian Forest.

The Hf isotope compositions of the redwitzites are close to chondritic values (Figs. 4, 5). Source heterogeneity was inferred for the redwitzites based on prominent variation of Sr and Nd bulk rock isotope composition (Holl et al. 1989; Siebel et al. 1995). This was explained by a mixing

relationship between gabbroic and granitic end-members. Source heterogeneity, however, is not clearly seen in the Hf–Nd data array but this could be due to the limited number of investigated samples ($n = 3$). If the granitic end member had a crustal isotope signature, a relatively depleted component is required to explain the chondritic isotope characteristics of the redwitzites. In terms of the mixing model, this would imply that the redwitzites comprise a blend of depleted mantle and enriched (crustal) material. Hence, as opposed to intermediate granites, the isotopic composition of the redwitzites does not point towards the involvement of an enriched mantle source.

Tracking magmatic processes (fractional crystallization, assimilation)

A key question in magma genesis concerns the ultimate reason for compositional variation. Fractional crystallization and crustal assimilation are the most important physical mechanisms of melt differentiation but often it is not straightforward to identify the prevalent process (e.g. Kemp and Hawkesworth 2003). The range of Hf isotope ratios obtained from a melt-precipitated zircon population of a single sample can help to evaluate this subject because it gives important information about the isotopic homogeneity of the melt from which the zircons grew (Griffin et al. 2002; Belousova et al. 2006; Kemp et al. 2005, 2007). The Leuchtenberg granite has long been regarded as an outstanding example of closed system fractional crystallization (Madel 1968; Siebel 1995). The three samples from the Leuchtenberg granite, which were investigated in this study, come from differently evolved parts of this pluton. The major and trace element characteristics of unfractionated sample Leu18 ($SiO_2 = 67.4$ wt%, Rb/Sr = 0.7) are controlled by the nature of the source materials whereas sample Leu2 ($SiO_2 = 74.8$ wt%, Rb/Sr = 3.5) reflects a higher degree of fractional crystallization (or assimilation). These two and a third intermediate sample from the Leuchtenberg granite (Leu6a, $SiO_2 = 71.5$ wt%, Rb/Sr = 1.2) have overlapping Hf isotopic compositions [εHf(t) Leu18 = − 1.33 ± 2.30, Leu6a = –0.49 ± 2.14, Leu2 = –1.00 ± 2.46] confirming that the magma of the Leuchtenberg granite underwent closed-system fractionation without major assimilation processes.

The porphyritic dykes of the southern Bavarian Forest contain zircons with a range in $^{176}Hf/^{177}Hf$ (up to ten ε-units), significantly larger than the analytical uncertainties (equivalent to ±1.1 ε-units). This grain-to-grain variation is also reflected by the high standard deviations in the dyke samples StDr2 and HzDr1 (Table 3). Zircons from the dykes form a homogeneous population and the CL images did not yield any evidence for pre-magmatic core material in the investigated samples (Fig. 6). A

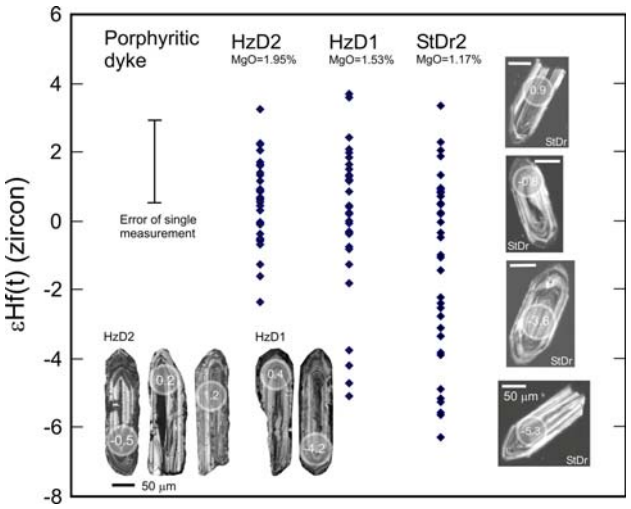

Fig. 6 Hf isotope composition of melt-precipitated zircons from three different samples of porphyritic dykes. Increase in data dispersion can be observed from sample HzD2 through HzD1 to sample StDr2. All samples are characterized by similar morphological zircon types and internal structures of these grains (CL images) do not show evidence for inherited material. *Circles* on CL images indicate locations of laser spots (all ~63 m in diameter) and corresponding εHf(t) values

concomitant U–Pb study identified a single age population at 299 ± 2 Ma in dyke sample HzDr2 (Propach et al. 2008) and no evidence for pre-magmatic zircon growth was found. This suggests that the zircons largely precipitated from a melt. Given the small grain size of the zircons, spatial resolution was not sufficient to evaluate intra-crystal isotope variability. However, the variation in Hf isotope composition of different grains from the same sample indicates an open system process. The dyke swarm ranges in composition from basaltic andesite to dacite and the spectrum of rock types was explained by magma mixing (Propach et al. 2008). If the dykes originated from a mantle-derived melt that was modified by fusion and assimilation of crustal rocks, this process should be recorded in the Hf-isotope composition of the zircons. In all three dyke samples, some zircons extend to positive, mantle-like εHf values around +3, indicating that the parental mafic magma was derived from a depleted mantle source. During assimilation, the release of Hf from crustal rocks can take place either by entrapment or by dissolution of zircons, or other Hf-bearing minerals and this process would modify the Hf isotope composition of the melt towards less radiogenic Hf ratios. If such process takes place during concomitant zircon crystallization, the Hf isotope composition of this mineral would likely record this process. The unradiogenic εHf values as low as –5 to –6 measured in some zircons of dyke samples HzD1 and StDr2 can be interpreted as a result of progressive assimilation of the melt by crustal material.

Conclusions

This study shows the feasibility to explore the origin of metaluminous and peraluminous (S-type) granitoids using in situ Hf data from melt-precipitated (i.e. non-inherited) zircons. To avoid pre-magmatic zircons from analyses careful monitoring by CL is a prerequisite in order to identify grains without discernible cores and a single-phase growth history appropriate for analysis.

Hf analysis of melt-precipitated zircons offers insights into the production of granitoids of the Bavarian Forest and the contributions of different granitoid source rocks. The data show that the texturally and geochemically different intrusions were derived from various crustal and mantle sources. In combination with geochemical and Nd-isotope data, single-grain Hf analysis of zircons provides a sensitive tool for tracing the involvement of both enriched and depleted mantle material and crustal components in these rocks.

Hf data on magmatic zircons can provide important additional constraints for the processes operating during magma crystallization (i.e. differentiation or crustal contamination processes). It is documented that in certain granites (Leuchtenberg, Tittling) geochemical variation was achieved under closed-system conditions during crystallization. On the other hand, porphyritic dykes contain zircons with a range in εHf(t) significantly larger than the analytical uncertainties. This reflects an open-system behavior probably caused by crustal assimilation processes of a mantle melt. Such insights would be easily camouflaged by whole-rock geochemical or isotopic studies.

Acknowledgments Research on Hf-in zircon analyses was funded by the Robert-Bosch Stiftung. Wang Fang, Katja Hannig, Wolfgang Reiter, Kai Hettmann, Liewen Xie and Yueheng Yang were instrumental for CL and Hf isotopic measurements. Gisela Bartholomä and Indra Gill-Kopp are thanked for zircon preparation and Elmar Reitter for Nd isotopic measurements. We thank Ulrich Teipel and an anonymous reviewer for insightful comments, which markedly improved the manuscript.

References

Andersen T, Griffin WL (2004) Lu–Hf and U–Pb isotope systematics of zircons from the Storgangen intrusion, Rogaland intrusive complex, SW Norway: implications for the composition and evolution of Precambrian lower crust in the Baltic shield. Lithos 73:271–288. doi:10.1016/j.lithos.2003.12.010

Augustsson C, Münker C, Bahlburg H, Fanning CM (2006) Provenance of late Palaeozoic metasediments of the SW South American Gondwana margin: a combined U–Pb and Hf-isotope study of single detrital zircons. J Geol Soc London 163:983–995. doi:10.1144/0016-76492005-149

Belousova EA, Griffin WL, O'Reilly S (2006) Zircon crystal morphology, trace element signatures and Hf isotope composition as a tool for petrogenetic modeling: examples from eastern Australian granitoids. J Petrol 47:329–353. doi:10.1093/petrology/egi077

Bouvier A, Vervoort JD, Patchett PJ (2008) The Lu–Hf and Sm–Nd isotopic composition of CHUR: constraints from unequilibrated chondrites and implications for the bulk composition of terrestrial planets. Earth Planet Sci Lett 273:48–57. doi:10.1016/j.epsl.2008.06.010

Chauvel C, Blichert-Toft J (2001) A hafnium isotope and trace element perspective on melting of the depleted mantle. Earth Planet Sci Lett 190:137–151. doi:10.1016/S0012-821X(01)00379-X

Chen F, Siebel W (2004) Zircon and titanite geochronology of the Fürstenstein granite massif, Bavarian Forest, NW Bohemian Massif: Pulses of late Variscan magmatic activity. Eur J Mineral 16:777–788. doi:10.1127/0935-1221/2004/0016-0777

Chu NC, Taylor RN, Chavagnac V, Nesbitt RW, Boella RM, Milton JA, German C, Bayon G, Burton M (2002) Hf isotope ratio analysis using multi-collector inductively coupled plasma mass spectrometry: an evaluation of isobaric interference corrections. J Anal At Spectrom 17:1567–1574. doi:10.1039/b206707b

Finger F, Gerdes A, Janoušek V, René M, Riegler G (2007) Resolving the Variscan evolution of the Moldanubian sector of the Bohemian Massif: the significance of the Bavarian and the Moravo-Moldanubian tectonometamorphic phases. J Geosci (Prague) 52:9–28. doi:10.3190/jgeosci.005

Flowerdew MJ, Millar IL, Vaughan APM, Horstwood MSA, Fanning CM (2006) The source of granitic gneisses and migmatites in the Antarctic peninsular: a combined U–Pb SHRIMP and laser ablation Hf isotope study of complex zircons. Contrib Mineral Petrol 151:751–768. doi:10.1007/s00410-006-0091-6

Flowerdew MJ, Millar IL, Curtis ML, Vaughan APM, Horstwood MSA, Whitehouse MJ, Fanning CM (2007) Combined U–Pb geochronology and Hf isotope geochemistry of detrital zircons from early Paleozoic sedimentary rocks, Ellsworth-Whitmore Mountains block, Antarctica. Geol Soc Am Bull 119:275–288. doi:10.1130/B25891.1

Franke W (2000) The mid-European segment of the Variscides: tectonostratigraphic units, terrane boundaries and plate tectonic evolution. In: Franke W, Haak V, Oncken O, Tanner D (eds) Orogenic processes: quantification and modelling in the Variscan belt. Geol Soc London, Spec Publ 179:35–61

Frentzel A (1911) Das Passauer Granitmassiv. Geognostisches Jahrb 24:31

Gerdes A, Zeh A (2006) Combined U–Pb and Hf isotope LA-(MC-)ICP-MS analyses of detrital zircons: comparison with SHRIMP and new constraints for the provenance and age of an Armorican metasediment in central Germany. Earth Planet Sci Lett 249:47–61. doi:10.1016/j.epsl.2006.06.039

Goodge JW, Vervoort JD (2006) Origin of Mesoproterozoic A-type granites in Laurentia: Hf isotope evidence. Earth Planet Sci Lett 243:711–731. doi:10.1016/j.epsl.2006.01.040

Griffin WL, Pearson NJ, Belousova E, Jackson SE, van Achterbergh E, O'Reilly SY, Shee SR (2000) The Hf isotope composition of cratonic mantle: LAM-MC-ICPMS analysis of zircon megacrysts in kimberlites. Geochim Cosmochim Acta 64:133–147. doi:10.1016/S0016-7037(99)00343-9

Griffin WL, Wang X, Jackson SE, Pearson NJ, O'Reilly SY (2002) Zircon geochemistry and magma mixing, SE China: in situ analysis of Hf isotopes, Tonglu and Pingtan igneous complexes. Lithos 61:237–269. doi:10.1016/S0024-4937(02)00082-8

Hanchar JM, Hoskin PWO (2003) Zircon. Rev Mineral Geochem 53:500. doi:10.2113/0530089

Harrison TM, Blichert-Toft J, Müller W, Albarède F, Holden P, Mojzsis SJ (2005) Heterogeneous Hadean hafnium: evidence of continental crust at 4.4 to 4.5 Ga. Science 310:1947–1950. doi:10.1126/science.1117926

Hawkesworth CJ, Kemp AIS (2006) Using hafnium and oxygen in zircons to unravel the record of crustal evolution. Chem Geol 226:144–162. doi:10.1016/j.chemgeo.2005.09.018

Holl KP, von Drach V, Müller-Sohnius D, Köhler H (1989) Caledonian ages in Variscan rocks: Rb–Sr and Sm–Nd isotope variations in dioritic intrusives from the northwestern Bohemian Massif, West Germany. Tectonophysics 157:179–194. doi:10.1016/0040-1951(89)90349-1

Holub FV, Klečka M, Matějka D (1995) Igneous activity. In: Dallmeyer RD, Franke W, Weber K (eds) Pre-Permian geology of central and eastern Europe. Springer, Berlin, pp 444–452

Hoskin PWO, Schaltegger U (2003) The composition of zircon and igneous and metamorphic petrogenesis. In: Hanchar JM, Hoskin PWO (eds) Zircon. Rev Mineral Geochem 53:27–62

Iizuka T, Hirata T (2005) Improvements of precision and accuracy in in situ Hf isotope microanalysis of zircons using the laser-ablation MC-ICPMS technique. Chem Geol 220:121–137. doi:10.1016/j.chemgeo.2005.03.010

Janoušek V, Gerdes A (2003) Timing the magmatic activity within the Central Bohemian Pluton, Czech Republic: conventional U–Pb ages for the Sázava and Tábor intrusions and their geotectonic significance. J Czech Geol Soc 48:70–71

Kalt A, Corfu F, Wijbrans JR (2000) Time calibration of a P–T path from a Variscan high-temperature low-pressure metamorphic complex (Bayerische Wald, Germany), and the detection of inherited monazite. Contrib Mineral Petrol 138:143–163. doi:10.1007/s004100050014

Kemp AIS, Hawkesworth CJ (2003) Granitic perspectives on the generation of secular evolution of the continental crust. In: Rudnick RL (ed) The crust. Treat Geochem 3:349–410

Kemp AIS, Wormald RJ, Whitehouse MJ, Price RC (2005) Hf isotopes in zircon reveal contrasting sources and crystallization histories for alkaline to peralkaline granites of Temora, south-eastern Australia. Geology 33:797–800. doi:10.1130/G21706.1

Kemp AIS, Hawkesworth CJ, Foster GL, Paterson GA, Woodhead JD, Hergt JM, Gray CM, Whitehouse MJ (2007) Magmatic and crustal differentiation history of granitic rocks from Hf–O isotopes in zircon. Science 315:980–983. doi:10.1126/science.1136154

Kinny PD, Maas R (2003) Lu–Hf and Sm–Nd isotope systems in zircon. In: Hanchar JM, Hoskin PWO (eds) Zircon. Rev Mineral Geochem 53:327–341

Klein P, Kiehm S, Siebel W, Shang CK, Rohrmüller J, Dörr S, Zulauf G (2008) Age and emplacement of late-Variscan granites of the western Bohemian Massif with main focus on the Hauzenberg granitoids (European Variscides, Germany). Lithos 102:478–507. doi:10.1016/j.lithos.2007.07.025

Köhler H, Müller-Sohnius D (1986) Rb–Sr-Altersbestimmungen und Sr-Isotopensystematik an Gesteinen des Regensburger Waldes (Moldanubikum NE Bayern)—Teil 2: Intrusivgesteine. N Jb Miner Abh 155:219–241

Kováříkova P, Siebel W, Jelínek E, Stemprok M, Kachlík V, Holub FV, Blecha V (2007) Petrology and geochemistry of redwitzites from Abertamy in the Nejdek-Eibenstock granite massif of the Krusné hory/Erzgebirge granite batholith, Czech Republic: its bearing on batholith genesis. Chem Erde 67:151–174. doi:10.1016/j.chemer.2007.04.002

Kroner U, Hahn T, Romer RL, Linnemann U (2007) The Variscan orogeny in the Saxo-Thuringian zone—heterogenous overprint of Cadomian/Paleozoic peri-Gondwana crust. In: Linnemann U, Nance RD, Kraft P, Zulauf G (eds) The evolution of the Rheic ocean: from Avalonian–Cadomian active margin to Alleghenian–Variscan collision. Geol Soc Am Spec Pap 423:153–172

Li QL, Chen F, Guo JH, Li YH, Yang YH, Siebel W (2007a) Zircon ages and Nd–Hf isotopic composition of the Zhaertai Group (inner Mongolia): evidence for early Proterozoic evolution of the northern North China block. J Asian Earth Sci 30:573–590. doi:10.1016/j.jseaes.2007.01.006

Li XH, Chen F, Guo JH, Li QL, Xie LW, Siebel W (2007b) Provenance of the low-grade Penglai Group in the Sulu UHP orogenic belt, eastern China: evidence from detrital zircon age and Nd–Hf composition. Geochem J 41:29–45

Liew TC, Hofmann AW (1988) Precambrian crustal components, plutonic associations, plate environment of the Hercynian fold belt of central Europe: indications from a Nd and Sr isotopic study. Contrib Mineral Petrol 98:129–138. doi:10.1007/BF00402106

Machado N, Simonetti A (2001) U–Pb dating and Hf isotopic composition of zircon by laser ablation MC-ICP-MS. In: Sylvester P (ed) Laser ablation-ICPMS in the earth sciences: principles and applications. St. John's, Newfoundland. Mineral Ass Can 29:121–146

Madel J (1968) Geochemical structures in a multiple intrusion granite massif. N Jb Miner Abh 124:103–127

Nebel O, Nebel-Jacobsen Y, Mezger K, Berndt J (2007) Initial Hf isotope compositions in magmatic zircon from early Proterozoic rocks from the Gawler Craton, Australia: a test for zircon model ages. Chem Geol 241:23–37. doi:10.1016/j.chemgeo.2007.02.008

Propach G, Bayer B, Chen F, Frank C, Hölzl S, Hofmann B, Köhler H, Siebel W, Troll G (2008) Geochemistry and petrology of late Variscan magmatic dykes of the Bavarian Forest, Germany. Geol Bavarica 110:304–342

Rudnick RL, Gao S (2003) Composition of the continental crust. In: Rudnick RL (ed) The crust. Treatise in Geochemistry 3:1–64

Scherer E, Münker C, Mezger K (2001) Calibration of the Lutetium–Hafnium clock. Science 293:683–687. doi:10.1126/science.1061372

Scherer E, Whitehouse MJ, Münker C (2007) Zircon as a monitor of crustal growth. Elements 3:19–24. doi:10.2113/gselements.3.1.19

Siebel W (1994) Inferences about magma mixing and thermal events from isotopic variations in redwitzites near the KTB site. KTB-Report 94–3:157–164

Siebel W (1995) Anticorrelated Rb–Sr and K–Ar age discordances, Leuchtenberg granite, NE Bavaria, Germany. Contrib Mineral Petrol 120:197–211. doi:10.1007/BF00287117

Siebel W, Höhndorf A, Wendt I (1995) Origin of late Variscan granitoids from NE Bavaria, Germany, exemplified by REE and Nd isotope systematics. Chem Geol 125:249–270. doi:10.1016/0009-2541(95)00083-X

Siebel W, Trzebski R, Stettner G, Hecht L, Casten U, Höhndorf A, Müller P (1997) Granitoid magmatism of the NW Bohemian Massif revealed: gravity data, composition, age relations, and phase concept. Int J Earth Sci 86:S45–S63 Geol Rundsch

Siebel W, Chen F, Satir M (2003) Late Variscan magmatism revisited: new implications from Pb-evaporation zircon ages on the emplacement of redwitzites and granites in NE Bavaria. Int J Earth Sci 92:36–53. Geol Rundsch. doi:10.1007/s00531-003-0348-5

Siebel W, Blaha U, Chen F, Rohrmüller J (2005) Geochronology and geochemistry of a dyke-host rock association and implications for the formation of the Bavarian Pfahl shear zone, Bohemian Massif. Int J Earth Sci 94:8–23. Geol Rundsch. doi:10.1007/s00531-004-0445-0

Siebel W, Hann HP, Shang CK, Rohrmüller J, Chen F (2006a) Coeval late-Variscan emplacement of granitic rocks: an example from the Regensburger Wald, NE Bavaria. N Jb Miner 183:13–26. doi:10.1127/0077-7757/2006/0058

Siebel W, Thiel M, Chen F (2006b) Zircon geochronology and compositional record of late- to post-kinematic granitoids associated with the Bavarian Pfahl zone (Bavarian Forest). Mineral Petrol 86:45–62. doi:10.1007/s00710-005-0091-7

Siebel W, Shang CK, Reitter E, Rohrmüller J, Breiter K (2008) Two distinctive granite suites in the south-western Bohemian Massif and their record of emplacement: constraints from zircon $^{207}Pb/^{206}Pb$ chronology and geochemistry. J Petrol 49:1853–1872. doi:10.1093/petrology/egn049

Streckeisen A (1976) To each plutonic rock its proper name. Earth Sci Rev 12:1–33. doi:10.1016/0012-8252(76)90052-0

Tait J, Schätz M, Bachtadse V, Soffel H (2000) Palaeomagnetism and Palaeozoic palaeo-geography of Gondwana and European terranes. In: Franke W, Haak V, Oncken O, Tanner D (eds) Orogenic processes: quantification and modelling in the Variscan belt. Geol Soc London, Spec Publ 179:21–34

Thirlwall MF, Walder AJ (1995) In situ hafnium isotope ratio analysis of zircon by inductively coupled plasma multiple collector mass spectrometry. Chem Geol 122:241–247. doi:10.1016/0009-2541(95)00003-5

Troll G (1968) Gliederung der redwitzitischen Gesteine Bayerns nach Stoff- und Gefügemerkmalen. Teil I: Die Typlokalität von Marktredwitz in Oberfranken. Bayer Akad Wiss Abh 133:1–86

Vervoort JD, Patchett PJ (1996) Behavior of hafnium and neodymium isotopes in the crust: constraints from Precambrian crustally derived granites. Geochim Cosmochim Acta 60:3717–3733. doi:10.1016/0016-7037(96)00201-3

Vervoort JD, Patchett PJ, Blichert-Toft J, Albarède F (1999) Relationships between Lu–Hf and Sm–Nd isotopic systems in the global sedimentary system. Earth Planet Sci Lett 168:79–99. doi:10.1016/S0012-821X(99)00047-3

Vervoort JD, Patchett PJ, Söderlund U, Baker M (2004) Isotopic composition of Yb and the determination of Lu concentrations and Lu/Hf ratios by isotopic dilution using MC-ICPMS. Geochem Geophys Geosyst 5:Q11002. doi:10.1029/2004GC000721

White AJR, Chappell BW (1977) Ultrametamorphism and granitoid genesis. Tectonophysics 43:7–22. doi:10.1016/0040-1951(77)90003-8

Willmann K (1920) Die Redwitzite, eine neue Gruppe von granitischen Lamprophyren. Z Dt Geol Ges 71:1–33

Woodhead J, Hergt J, Shelley M, Eggins S, Kemp R (2004) Zircon Hf-isotope analysis with an excimer laser, depth profiling, ablation of complex geometries, and concomitant age estimation. Chem Geol 209:121–135. doi:10.1016/j.chemgeo.2004.04.026

Wu FY, Yang YH, Xie LW, Yang JH, Xu P (2006) Hf isotopic composition of the standard zircons and baddeleyites used for U–Pb geochronology. Chem Geol 234:105–126. doi:10.1016/j.chemgeo.2006.05.003

Žák J, Holub FV, Verner K (2005) Tectonic evolution of a continental magmatic arc from transpression in the upper crust to exhumation of mid-crustal orogenic root recorded by episodically emplaced plutons: the central bohemian plutonic complex (Bohemian Massif). Int J Earth Sci (Geol Rundsch) 94:385–400

Zeh A, Gerdes A, Klemd R, Barton JM (2007) Archaean to Proterozoic crustal evolution in the central zone of the Limpopo belt (South Africa–Botswana): constraints from combined U–Pb and Lu–Hf isotope analyses of zircon. J Petrol 48:1605–1639